

GRAPHENE CHANNEL FIELD EFFECT TRANSISTORS
FOR BIOSENSING APPLICATIONS

A Thesis

Presented to the Faculty of the Graduate School

of Cornell university

in Partial Fulfillment of the Requirements of the Degree of

Master of Science

by

Aniket Kakatkar

May 2014

© 2014 Aniket Kakatkar

ABSTRACT

Bio-sensing and analysis is an important step in the lab-on-a-chip paradigm. We develop high-throughput, multi-channel, large area graphene channel field effect transistors with enhanced sensitivity for biomolecule detection exploiting the excellent electrical and biocompatible nature of graphene. Till date biosensors using graphene have been too small as they use exfoliated graphene. Large area scaling of graphene biosensors increases sensing area and sensitivity. So we investigate the possibility of CVD graphene being an effective platform for biomolecule detection.

In the present thesis, we explain how our device allows larger changes in the electrical output for enhanced sensitivity and how our novel contamination free graphene transfer technique and new approaches to device design and fabrication make our sensor devices successful. We explain underlying mechanisms behind biomolecule detection through graphene functionalization. We also present an array of biosensors, enabling detection of multiple biomolecules simultaneously. Finally, we present possible development roadmaps for our sensors.

BIOGRAPHICAL SKETCH

Aniket Kakatkar was awarded a Bachelor of Technology degree in Engineering Physics from the Indian Institute of Technology (IIT) – Delhi in 2012. Subsequently, he joined the Master of Science program in the School of Applied and Engineering Physics at Cornell University.

Aniket has been the recipient of numerous and prestigious awards including the National Talent Search Examination Scholarship from the Government of India and the Summer Undergraduate Research Award from IIT Delhi.

Aniket is interested in the semiconductor device physics and manufacturing technologies. In addition to exploring the world of semiconductors through a focus on the Nanotechnology track during his Master's degree, he has also completed an internship at GLOBALFOUNDRIES, Malta, NY working on process flow material development for the 20nm IC technology node. After completing his graduate degree, Aniket will move to Saratoga, New York where he will join GLOBALFOUNDRIES as a full-time employee in the Technology Development and Research team.

Aniket's thesis, "Graphene Channel Field Effect Transistors for Biosensing Applications" was supervised by Dr. Harold Craighead.

ACKNOWLEDGEMENTS

I take this opportunity to thank all those without whom this thesis couldn't have been completed and show my gratitude to all those who have constantly helped and guided me throughout the project.

First and foremost, Prof. Harold Craighead, School of Applied and Engineering Physics at Cornell University – for giving me the opportunity to work on this thesis and also the constant help, advice and motivation to achieve the desired objectives. I would also like to thank Prof. Manfred Lindau, my second committee member for his kind guidance and support.

I would like to show my greatest appreciation to Abhilash Thanniyil Sebastian. I cannot thank him enough for his help. Without his guidance and encouragement this project would not have materialized. In addition, I would also like to thank Prof. Jeevak Parpia and members of his group Robert de Alba and Nikolay Zhelev for their timely advice and help. I am most grateful to Kylan Szeto, Jiawei Yeh and Jaime Benitez-Marzan from the Craighead group as well as the staff at the Cornell Nanofabrication Facility and Peter Rose from the McEuen Group for their seasoned advice and immense help. Lastly, I would also like to thank my friends and family for their unconditional support and encouragement.

Of course, the responsibility for any errors or inadequacies in this thesis is entirely my own.

TABLE OF CONTENTS

Biographical Sketch	iii
Acknowledgements	iv
Table of Contents	v
List of Figures	vii
1. Introduction and Motivation	01
2. Theoretical Background	03
2.1 Bio-sensing and Field Effect Transistors	03
2.2 Graphene and its Properties	04
2.2.1 Electrical Properties	06
2.2.2 Graphene as a Biocompatible Material	08
2.2.3 Functionalization of Graphene	09
2.2.3.1 Functionalization through Covalent Binding.	10
2.2.3.2 Functionalization through Non-covalent Adsorption.	10
2.2.3.3 CVD Graphene and Functionalization.	12
2.3 Approaches to Biomolecule Detection	13
2.4 Our Approach: GraFETs for Bio-Sensing	15
2.4.1 Device for Specific Biomolecule Detection	15
2.4.2 Specific Biomolecules for Detection	16
3. Experimental Methods	18
3.1 Graphene Growth	18

3.2 Device Fabrication	19
3.3 Graphene Transfer	20
3.4 Metal Insulation	24
3.5 Device Testing	26
4. Results and Discussion	28
4.1 Graphene Growth Characterization	28
4.1.1 Simple Oxidation Test	28
4.1.2 Scanning Electron Microscope Imaging	29
4.1.3 Raman Spectrum	31
4.2 GraFET Characterization	32
4.2.1 I-V Characteristics of GraFET devices	32
4.2.2 Resistance Measurements of GraFET devices	33
4.3 Demonstration of Dirac Point and its Tunability	34
4.4 Specific Biomolecule Detection	36
4.4.1 Functionalization behind Mechanism –Langmuir Model	38
4.5 An Array of GraFET sensors	40
5. Conclusions and Future Work	43
5.1 Conclusions	43
5.2 Scope for Future Work	44
References	45

LIST OF FIGURES

1. Schematic Illustration of GraFET device	01
2. Schematic Illustration of 2 Dimensional Graphene	05
3. Schematic Illustration of Electric Properties of Graphene	07
4. Schematic Illustration of Graphene Functionalization	11
5. GraFET device design	20
6. Schematic Illustration of Contamination Free Graphene Transfer	21
7. Schematic Illustration Final GraFET device with characterization details	25
8. Simple Oxidation Test for Graphene Growth – Optical Microscope Image.	27
9. SEM Image of Partial Graphene Growth	28
10. SEM Image of Multilayer Graphene Growth	29
11. SEM Image of Single Layer Graphene Growth	29
12. Raman Spectrum of Graphene	30
13. I-V Characteristics of GraFET devices	31
14. Contact Resistance extraction from GraFET devices	32
15. Demonstration of Dirac Point in CVD Graphene and its Tunable Nature	34
16. Detection of Lysine using GraFETs	35
17. Detection of Bovine Serum Albumin using GraFETs	36
18. Evidence of Functionalization due to Lysine through Binding Curves	38
19. Evidence of Functionalization due to BSA through Binding Curves	39
20. An Array of GraFET sensors	40

Chapter 1

Introduction and Motivation

Contemporary scientific research often transcends just academic curiosity and is now more than ever increasingly translated into the real-world impact potential of such research. The two fields of biology and electronics that have long had a huge impact on the real world are now interacting due to the enabling platform that is nanotechnology. This field, referred to as bioelectronics, looks at the flow of information both from electronics to biology (bio-actuation) or from biology to electronics (bio-sensing). One important area where the synergy between biology and electronics will come to fruition sooner than later is the lab-on-a-chip approach. Lab-on-chip devices, which are akin to Integrated Chips of the semiconductor industry, are built to perform various functions on the same chip platform. Bioelectronics through the lab-on-chip approach allows for immediate biological agent detection and sensing of particular biomolecules.

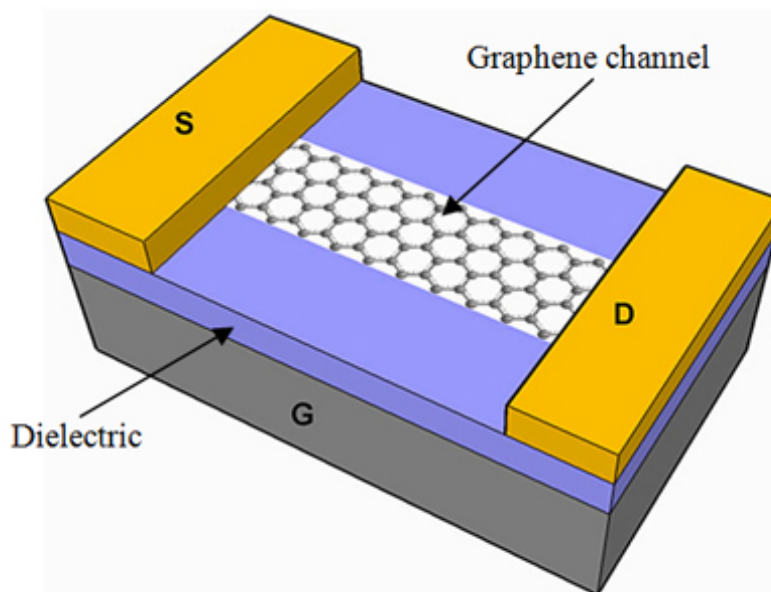


Figure 1 Schematic Illustration of GraFET device - S: source, D: drain, G: back gate. (adapted from Tejas Deshpande, Technophilic Magazine, Feb. 7, 2011)

This specifically motivates our research and in the present thesis, we present the development and functionality of a Graphene Channel Field Effect Transistor (abbreviated as GraFET) as a bioelectronics sensor. A schematic of a GraFET device is shown in Figure [1]. Our sensor device uses graphene as the crucial material for the platform for protein biomolecule detection. We shall look at graphene and some of its properties that make it so useful in bioelectronics in Chapter 2. In Chapter 2 we will also discuss the protein-graphene interaction, here onwards referred to as the functionalization of the graphene surface (by the proteins), the specific proteins that we test and the principle of working of our GraFET device. Having established this theoretical framework, we shall move on to the experimental procedure and device fabrication methods in Chapter 3. In Chapter 4, we will show the performance of our devices and present a discussion on the results obtained. Finally, we shall conclude with a brief summary and possibilities for future work in this area in Chapter 5.

Chapter 2

Theoretical Background

2.1 Bio-sensing and Field Effect Transistors

Bio-sensing in the field of bioelectronics is in essence transfer of information from biology to electronics. Once a primary signal from the biological agent or system is obtained, standard electronic systems and circuits exist that relay, manipulate and process this signal as desired. The critical element then in a biosensor device is the transducer that transfers the biological or chemical signal efficiently into an electric one. With the onset of lab-on-a-chip approach and the emphasis on immediate bio-agent detection, we now prefer a sensor device that apart from detecting biomolecules accurately also is easy to use for the end-user. One approach is to make use of traditional detection techniques [1]. However, these are expensive and slow as compared to the contemporary techniques used in bioelectronics. Another approach is the use of micro-electrode arrays (MEAs). These devices work in principle [2] but have problems in either functionality or in their shelf life [3].

The other approach for specific bio-agent detection is the use of nanoscale chemical field effect transistors abbreviated as ChemFETs. In a Field Effect Transistor (FET), an electric field controls the conductivity of a channel of charge carriers in a semiconductor system. This semiconductor is typically silicon, mainly as all necessary fabrication steps for FETs are those of standard semiconductor manufacturing technologies. ChemFET is merely a FET being used as a chemical or biological sensor.

Such FETs have already long been used in bioelectronics [4] and give better results than the aforementioned MEAs [5]. Yet the use of just silicon limits the electrical properties of these FETs [6]. So, the approach of the day, the one that we use, is that of replacing the conducting channel in the FET by a material that is better than silicon. Carbon nanotubes [7] and semiconductor heterostructures [8] have better electrical properties in some sense than silicon. Yet, their use in biological environments presents compatibility problems while the use of other materials leaves much to be desired from the performance of the sensor devices, particularly in real-life bio-environments. An alternative is the use of graphene as the channel material in field effect transistors [9-11]

2.2 Graphene and its Properties

Ever since its discovery graphene has attracted a vast amount of interest from the scientific community [12,13]. Graphene is one of the crystalline forms of carbon but what makes it remarkable is that graphene is a single planar sheet of carbon atoms. These carbon atoms are arranged in a hexagonal pattern in an sp^2 hybridized fashion and the carbon-carbon bonds with a bond length of 0.14nm are very strong. This inherent strength makes graphene a stable material and graphene, a truly two dimensional crystalline material has opened new vistas in science by providing the community with a new class of material. Indeed, The Nobel Prize in Physics, 2010 was awarded to Andre Geim and Konstantin Novoselov “for groundbreaking experiments regarding the two-dimensional material graphene” [14]. Graphene can be produced by micromechanical exfoliation or by reducing silicon carbide [15]. However, these techniques of graphene production impose a limit on the usable area of graphene.

Graphene growth on metal substrates through the technique of chemical vapor deposition [16] avoids this problem and graphene grown through this technique is now being extensively investigated for potential applications.

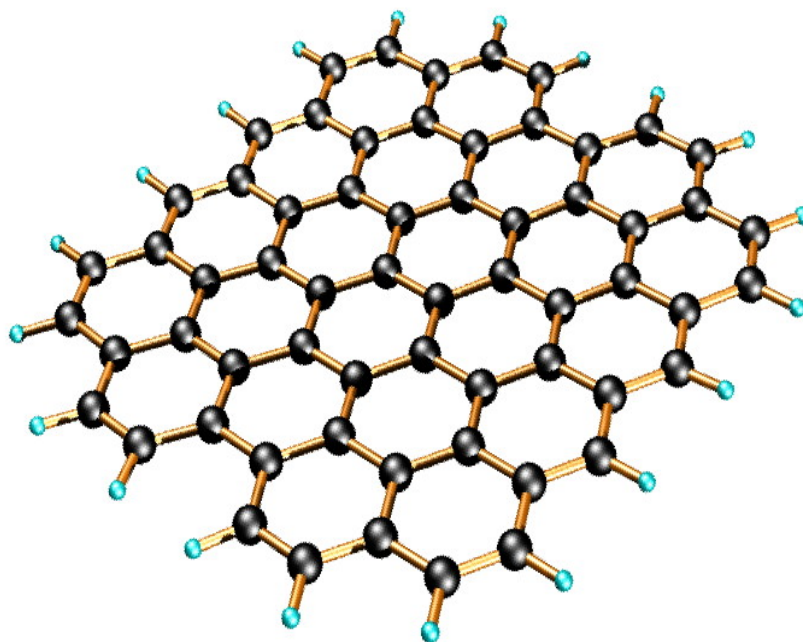


Figure 2: Schematic Illustration of sp^2 hybridized 2D material: graphene
(adapted from Hamilton, Barron – OpenStax College, Connexions, Rice University)

Graphene has useful optical [17,18] and thermal properties [19,20] yet its mechanical properties are one of the two that stand out. Stating these mechanical properties as remarkable does graphene great injustice for the 2D graphene sheet appears to be one of the strongest known materials to man [21]. Even the Nobel prize, 2010 announcement [22] states: “a 1 square meter graphene hammock would support a 4 kg cat but would weigh only as much as one of the cat's whiskers, at 0.77 mg”.

While these properties make graphene a remarkable material two other properties of graphene make it invaluable in the field of bioelectronics.

2.2.1 Electrical Properties

The first of these properties are the electric properties of graphene. Although the general discussion of electrical properties of graphene is a vast field on which a large amount of literature exists [6,10,12,13,23,24], we shall concentrate on only those properties that are of concern to bio-sensing. Firstly, graphene has extremely high electrical conductivity. Values of electron mobility of $15,000 \text{ cm}^2/\text{V}\cdot\text{sec}$ have been reported [12]. Also, unlike the case of silicon or gallium arsenide, both electrons and holes – the two types of charge carriers in semiconductors, have similar mobility. Furthermore, graphene is different from bulk or 3 dimensional materials in that it is a zero band gap material. In other words, graphene is a zero-gap semiconductor. The difference between a conventional semiconductor like silicon and a zero-gap semiconductor (graphene) is explained in Fig [3]. Figure [3a] shows the existence of a band gap in typical semiconductors while the band structure for graphene dictates that the top of the valence band and the bottom of the conduction band are at the same energy level at certain points in the Brillouin zone [23]. These points, where the conduction and valence bands meet are near the corners of the hexagonal Brillouin zone and are referred to as the Dirac Points [24]. We note that even if the energy gap for graphene is zero, there is no overlap between valence and conduction bands unlike the case for metals. Clearly at a Dirac Point, the density of charge carriers is zero and in a simplistic case we expect zero conduction at the Dirac Points. However, while the conduction does go to a minimum value at the Dirac point due the absence of charge carriers, the conductivity is not exactly zero. The reason for this non-zero minimum

conductivity is believed to be localized puddles of electrons [23] that may arise due to imperfections or rippling in the graphene sheet. This Dirac Point and the associated minimum in conduction becomes the central point in our biomolecule detection scheme whilst using graphene FETs.

Applying an external voltage can be used to detect the Dirac Point in graphene. This can be best understood using the concept of the Fermi level [25] that denotes the point at which the probability of electron occupying a state at the given energy level is 0.5. On applying voltages, the aforementioned occupancy probability changes and this results in a shift in the Fermi level in the graphene. This in turn controls the number of free carriers. At a certain applied voltage, the Fermi level reaches the Dirac point and

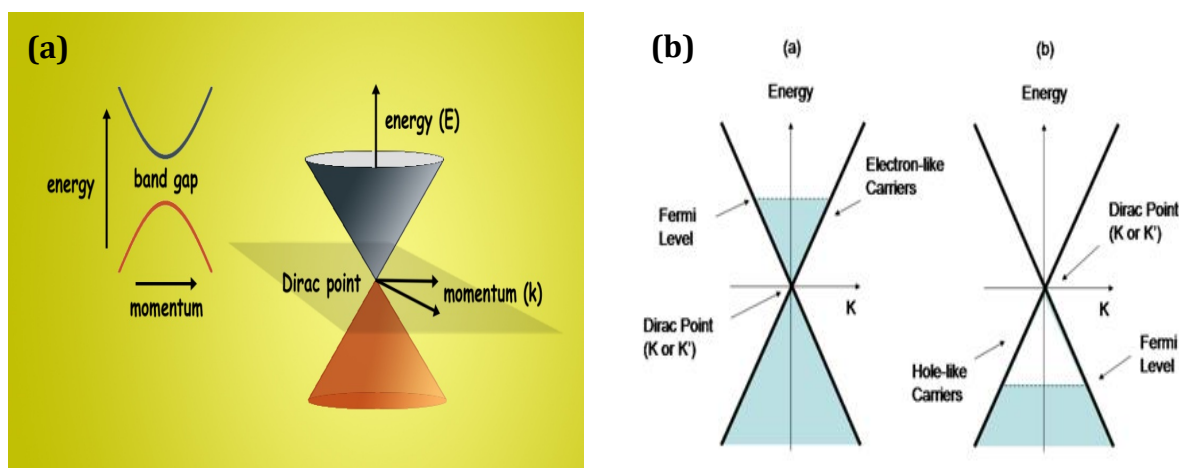


Figure 3 (a) E-k band diagram for a typical semiconductor (left) and that for zero and-gap graphene (right) - adapted from Lawrence Berkeley National Laboratory, Press Release, April 25, 2008 (b) Effect of Voltage on Fermi Level - electrons as charge carriers (left) and holes as charge carriers (right) - adapted from N. Stander, Stanford University, 2007

the conductivity is now minimal. The voltage at which this phenomenon occurs is called the Dirac voltage and is a direct indication of the Dirac Point in graphene. Clearly, at lower voltages, the Fermi level is in the valence band and conduction occurs through

holes as the charge carriers. On the other hand, at voltages greater than the Dirac voltage, the Fermi level is in the conduction band and electrons are majority charge carriers. Going away from the Dirac voltage, the number of charge carriers increases and the conductivity in turn increases. We shall use the terms Dirac voltage and Dirac point loosely as in most cases it will be clear to the reader that the Dirac Point in sensing refers to just the voltage at which the Dirac Point is observed. We also note that the Dirac Point depends on experimental conditions, the graphene surroundings and the substrates in question.

2.2.2 Graphene as a Biocompatible Material

The second and probably equally if not more important property of graphene that is extremely useful in bio-sensing is its biocompatibility [26]. If sensing experiments are to be done in real life aqueous environments or in certain cases in vivo, the stability and compatibility of the materials in use is vital. The biological environment is harsh and renders many materials unstable. Damages to the device and the resulting degraded device performance is indeed a concern but even more pressing is the damage done to the biological environment. Graphene is amongst the few materials that is stable in biological environments and does no damage to its surroundings [26]. The mechanical flexibility graphene offers is an additional advantage.

Other materials like carbon nanotubes also exhibit properties useful in bio-sensing but graphene has a better performance with respect to signal to noise ratio [27]. The sensitivity of graphene is also higher specially because the interactions between

graphene and the biomolecule to be detected occur on the surface and graphene being a planar sheet offers a larger sensing area than competing materials.

2.2.3 Functionalization of Graphene Surface

As already mentioned, graphene exhibits the Dirac Point and is biocompatible which makes it a great tool in biomolecule detection. But, the great potential of graphene in bio-sensing can only be harnessed by inducing signature changes in some property of the graphene. A good approach to this condition is to induce a change in the Dirac voltage or the Dirac point of graphene. Biomolecules often have a charge associated with them. When these biomolecules interact with graphene, the charge present on the biomolecule alters the electric properties of graphene. Specifically, it induces charged carriers in the graphene and the effect is to shift the Fermi level of graphene. Now, when external voltage is applied, the Fermi level corresponds to the Dirac point at a voltage different than for a graphene-only scenario. This difference in the voltage depends on the charge on the biomolecule. As the charge to molecular weight ratio and the degree of interaction with graphene is a signature property of specific biomolecules, the amount of voltage change caused because of the biomolecule is also a signature property of the biomolecule. By sensing this signature change in the Dirac Point or voltage electrically, the graphene surface is now made into a biosensor. The induced changes that give the graphene its special properties are said to functionalize the graphene. A great review of graphene functionalization may be found in Georgakilas et al. [28] and in Kuila et al. [29]

In general, Graphene may be functionalized either through covalent or non-covalent binding. Complex functionalization protocols have been developed [30] for graphene functionalization through biomolecules. Noting that such processes will be useful for certain specific biomolecules, we turn our attention to protein molecules that get easily adsorbed on the graphene surface to demonstrate that our approach is useful in bio-sensing. For our purposes specifically the protein molecules that we use, functionalization is obtained just by dipping our device in a solution of the protein in De-ionized (DI) water.

2.2.3.1 Functionalization through Covalent Binding

Covalently functionalizing graphene involves a change in the structure in the graphene sheet as some carbon atoms rehybridize from a sp^2 to a sp^3 state [28] Graphene functionalized this way usually involves a reaction with the functionalizing agent. Organic functional groups [31,32] and free radicals or diazonium salts [33,34] form covalent bonds with the graphene and extensive studies have been done in this area. However, in our case the specific biomolecules do not react with the graphene but rather bind to the surface because of adsorption in the surface.

2.2.3.2 Functionalization through Non-covalent Adsorption

Non-covalent functionalization of graphene typically involves the physical adsorption of the functionalizing agent on the graphene surface. Studies on non-covalent graphene functionalization have been done on graphitic oxides or exfoliated graphene in general as well as for specific biomolecule detection. [28,29,35-38] Biomolecules like proteins, DNA interact with graphene in this way. The interactions

between the biomolecule and the graphene typically are electrostatic or van der Waal force based and no chemical reaction occurs. The functionalizing agent that is adsorbed onto the graphene surface has some electric charge. This alters the electric properties of graphene and causes a shift in the Dirac point. Thus, a shift in the Dirac voltage is observed during a sweep of the external applied voltage. As mentioned before, this shift is dependent on the change in electric charge, the amount of binding etc. all of which are properties mainly of the biomolecule and of the interaction of the biomolecule and the graphene. So, depending on which biomolecule is used, a signature shift in the Dirac Point is observed which in turn may be used for to make an effective biosensor. An added advantage the non-covalent interaction offers is that the process is reversible. Graphene with molecules adsorbed onto it may be returned to its original state by gently heating [39]. This is of great advantage to us as after functionalization, if we rinse the sensor device with De-Ionized water and heat it, the graphene reverts back to its pre-functionalized stage thus making it possible to reversibly detect biomolecules. A schematic of the functionalized graphene surface is shown in Figure [4].

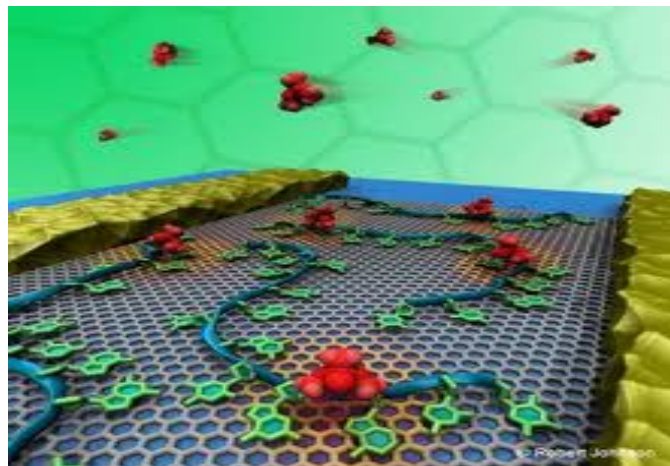


Figure 4 Schematic Illustration of graphene functionalization : biomolecules (red colored) shown functionalizing the hexagonal 2D graphene. On the sides are metal contacts (yellow) (adapted from [40])

2.2.3.3 CVD Graphene and Functionalization

As mentioned earlier, functionalized graphene can be used to detect biomolecules because of the shift in the Dirac Point that is a direct result of the functionalization. Most noteworthy functionalization experiments have been done on exfoliated graphene. As mentioned earlier, this presents an inherent limit on the scalability of sensor devices that make use of exfoliated graphene. The grain sizes are very small and even continuous graphene monolayers are only a few micrometers in size at best. CVD grown graphene is an obvious answer to the scalability and size problem as arbitrarily large graphene can be grown using CVD. And yet, till very recently no literature exists on CVD graphene being functionalized. One reason for this is that functionalization of graphene requires a near pristine and uniform graphene surface. While CVD graphene is scalable to large areas, it was not till very recently that a reliable method that gave uniform graphene monolayer coverage was reported [41]. Secondly, the graphene grown is on a metal substrate, typically copper for best properties [42,43]. To use this graphene in a FET, it must be transferred to the proper silicon substrate. Most of the known literature uses chemical etchants to etch away the copper [6,44] and then scoop the graphene onto the desired substrate. While this preserves many of the properties of graphene, we believe the use of such a transfer technique also contributes the disappearance of the Dirac Point. Residues from the transfer technique interfere with the clean graphene surface and we also believe that the dopants introduced from the ionic copper etchants uncontrollably contaminate the graphene. All these reasons are maybe why Saltzgaber et al. [44] is one of the very few

reports on Dirac Peaks being observed for CVD graphene in functionalization experiments.

However, we use a novel graphene transfer technique, inspired from the work of Gupta et al. [45] Their Soak and Peel Delamination (SPeeD) technique allows for graphene transfer without use of any chemical etchants. Though the method they suggest is an excellent transfer technique and may be used for MEMS devices or in suspended devices, the graphene surface is not clean enough for functionalization. However, basing our transfer technique off the idea of SPeeD, we have developed and optimized a transfer technique that not only avoids the exposure of CVD graphene to harsh chemicals but also gives a pristine clean surface. As will be shown in Chapter 3, the use of such a transfer technique on CVD grown graphene gives a Dirac Point and is thus available for functionalization.

2.3 Approaches to Biomolecule Detection

The use of using non-covalent functionalization of CVD graphene has only recently been reported. Garrido et al. [6] and Saltzgaber et al. [44] report changes in the Dirac Point of CVD graphene as a basis for biomolecule detection. In this approach, a field effect transistor is fabricated wherein the conducting channel is made of graphene. When a gate voltage is applied to functionalized graphene, the graphene channel conducts current according to the number of available carriers. When a sweep of the gate voltage is performed, an external voltage is effectively applied to the graphene. As mentioned earlier, this changes the number of carriers and thus the conductivity of the graphene channel. At the Dirac point, a conductivity minima and thus a current minima

is observed and the voltage at which this minimum occurs is detected. However, these devices are replete with a multitude of problems. The sensors are mostly small scale and this limits area available for functionalization and thus sensor performance. The gating mechanism of the transistor devices is also through solution that presents problems in itself. When gating is done through a solution the nature of the graphene-solution interface is crucial. This interface causes a significant potential drop that may not be accounted for in sensing experiments. When a gate voltage is applied, the charge in the graphene side is easily calculated using the induced carriers. But, in the solution phenomena like the surface effects, charge screening due to solution, possibility of hydrolysis and various other imbalances in the solution exist. The interface between graphene and the solution may be simulated using molecular dynamics simulations [46] and this shows an effective dielectric constant for water differing from the expected value. The extended Poisson-Boltzmann model then has to be used which further complicates matters [6]. Furthermore, the transfer techniques for graphene used in most literature is that of chemical etching which contaminates the graphene surface and may not truly reflect the real Dirac Point in graphene. Though only changes in Dirac voltages are to be recorded for sensing, we do not know if biomolecules interact with pristine and contaminated graphene in the same way. Lastly, these devices first transfer the graphene onto the wafer substrate and then pattern the metal contacts onto them. This exposes the graphene to needless chemicals and also increases the risk of imprecise alignments.

We stress that these complexities make true bio-sensing difficult. And hence, we present our novel approach for specific biomolecule detection using graphene channel field effect transistors or GraFETs.

2.4 Our Approach: GraFETs for Bio-sensing

We have identified that sensing area and solution based gating are two of the main concerns of using CVD grown graphene in GraFETs for biomolecule detection. Furthermore, the devices already reported are generally just a set of gated metal contacts – that is, just one device with low throughput capability. We present here a large area multi channel back-gated GraFET that results in significantly larger shifts in the Dirac Point due to functionalization. As a consequence, sensing performance of our GraFETs is better thus making them more effective sensors. Furthermore, as graphene transfer occurs post device fabrication, the issues of alignment and contamination are further reduced. In addition, the device design and sensing set up are very easy to use keeping in mind convenience of the end user.

2.4.1 Device for Specific Biomolecule Detection

The device consists of a set of inter-digitated electrodes as shown in Figure [5]. We note several important features of the device. Firstly, we fabricate an array of sensors on a single chip. The same sample of graphene, not just from the same growth but also the one that is exposed to the same treatments and thus the one that has undergone the same changes is used on a device chip. This avoids any changes introduced by variation in graphene properties in the different channels. The array of sensors might have channel lengths varying to as high as $200\mu m$. Various types of

devices with constant as well as varying channel lengths can be integrated into the same device. This makes possible the parallel detection of a number of proteins through a microfluidic channel approach thus enabling high throughput devices. Secondly, the gate voltage is applied through the back gate mechanism. In general back gating a device has an effect on speed of operation but since bio-functionalization timescales are greater than electronic delay timescales, this is not a bottleneck for our purposes. Back-gating the GraFETs avoids the use of solution gating thus getting rid of many problems associated with reported sensor devices. Voltage is not applied through an aqueous solution. So, the contact regions of the source and drain electrode do not need any kind of epoxy or other isolation while applying the voltage. This increases the ease of use of our sensor devices by a significant amount. We note however, that in our approach the metal electrodes if left bare and exposed to the environment of the solution in which the GraFET is dipped, have a solution-metal interaction that suppresses the graphene-biomolecule interaction. So, our approach needs either the metal to be covered by a resist or an insulating layer or the contact between metal and solution can be avoided by restricting the solution flow to the channel via the use of microfluidic channels. Other than this, the general mechanism behind the working of our GraFET devices is that of the shift in Dirac Point due to non-covalent functionalization of graphene due to specific biomolecules.

2.4.2 Specific Biomolecules for Detection

We use two biomolecules – Bovine Serum Albumin (BSA) and lysine as sample protein biomolecules that are to be detected. BSA is a globular protein derived from

cows. The mature BSA protein contains 583 amino acids and has a molecular weight of 66,463 Da [47]. BSA is a fairly standard protein biomolecule in laboratories and is used in immunohistochemistry, in enzyme linked immunosorbent assays (ELISA) and as a standard for protein concentrations [48]. Lysine on the other hand is an amino acid. The chemical formula for lysine is $\text{HO}_2\text{CCHNH}_2(\text{CH}_2)_4\text{NH}_2$ and it has a molar mass 146.19 g/mol [49]. Lysine is an essential amino acids for humans.

Both BSA and lysine that we used are from Sigma Aldrich and along with the associated ions, altogether have an associated positive charge. So, upon functionalization due to the positive charge, a greater amount of negative carriers need to be introduced in the channel to balance the charges and obtain the Dirac Point. Applying a greater back gate voltage does this. One can think of the mechanism as an inversion channel being introduced in the graphene. Alternatively, one may visualize the intermediate dielectric oxide between the silicon on which the voltage is applied and the graphene channel, resulting in a capacitor being formed. With any approach, the Dirac point gate voltage is expected to shift to higher (more positive) voltages because of functionalization due to BSA and lysine. Because at given concentrations, the binding (adsorption) and the specific charge of the proteins differs, the amount by which the voltage is expected to shift is different and thus can be used as an identifier to detect the biomolecule.

Chapter 3

Experimental Methods

3.1 Graphene Growth

To enable scaling of to arbitrarily large areas we employed the technique of chemical vapor deposition for growth of single layer graphene. This process occurs on a metal substrate and best results including uniform growth coverage by monolayers has been found for copper [41-43]. The basis for our recipe of graphene growth is developed in [41]. We used $20\mu\text{m}$ thick Copper sheets from Nilaco Corporation (Item Number 113213) and methane was used as the carbon source. A reduced pressure of 0.5 mTorr was created in the silica tube used for growth and the sample was annealed for 60 minutes at 1000 C in 60 SCCM of hydrogen. Methane and hydrogen in a ratio 3:5 were flown for a period of 20 minutes for actual growth. Later the furnace was let to cool down to below 100 C while still flowing the gas mixture. As an alternative, the ‘pita pocket’ or enclosure growth as suggested in [41] was also used for a few devices. As will be discussed in Chapter 4, if the graphene obtained through either the pita pocket growth or the previously mentioned ‘standard’ growth is uniformly monolayer, very similar Dirac Points are observed. In general, for ease of use and to keep the sample wrinkle free, the standard growth was favored over the pita pocket one.

The graphene sample was tested through a variety of ways including a simple substrate oxidation test, scanning electron microscopy (SEM) imaging and Raman Spectroscopy. To have a primary test of coverage, the sample was kept on a hot plate

pre-heated to and maintained at 250 C for 15 seconds. Bare copper, not covered by graphene, oxidizes readily to form red colored oxide while the graphene protects the copper beneath it from getting oxidized as easily. After a primary observation as discussed in Chapter 4, the copper is again kept on the hot plate for 2-3 minutes to observe bilayer patches. Samples having patchy and non-uniform growth or those that were heavily bi-layered were discarded. The remaining samples were tested using standard SEM imaging. Furthermore, Raman spectra of the samples were to taken to confirm graphene monolayers.

3.2 Device Fabrication

The devices used as graphene channel field effect transistors were fabricated on a p-doped Silicon wafer. The silicon wafer doping level was high so that the substrate would be adequately conducting to take electrical measurements through back gating. Silicon oxide was grown on the bare silicon substrate in a thermal oxidation furnace and was etched to have a resultant 300nm oxide acting as the insulator. Using a positive tone resist (MEGAPOSIT SPR 220 – 3.0 by Shipley Company) the desired device pattern as shown in Figure [5]. Arrays of inter-digitated source and drain electrodes were transferred lithographically on the aforementioned SiO₂/Si wafer using exposure times of 6 seconds (SUSS Micro Tech MA6 Aligner; wavelength 280 nm). The exposed resist was washed away in DI water after developing in a developer solution (AZ 726 MIF) for 90 seconds. Metal electrodes consisting of 10 nm Titanium (Ti) and 40nm Platinum (Pt) were deposited through an electron gun evaporation system (CVC SC4500). The Ti layer is used to promote adhesion and avoid the risk of platinum

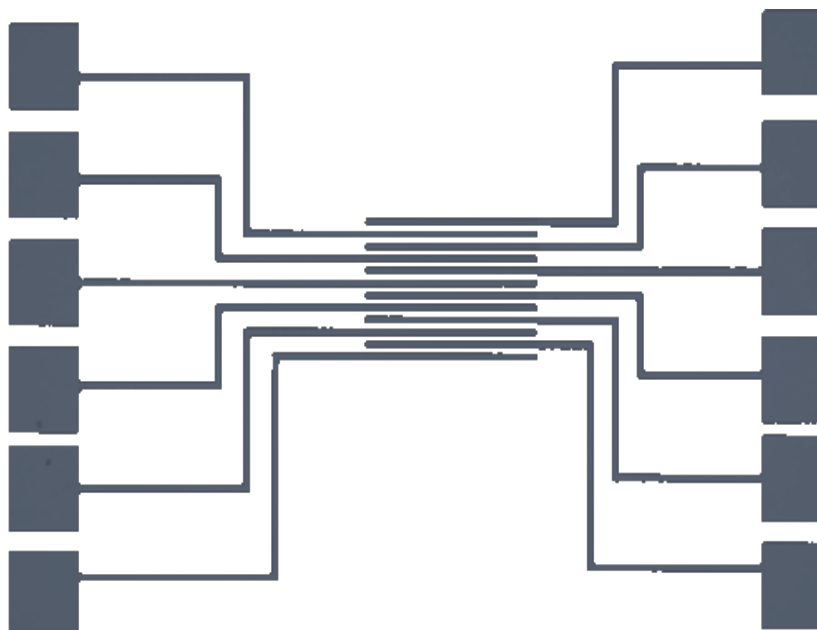


Figure 5 GraFET device design

flaking off during processing or testing of the devices. The entire sample was then kept overnight for liftoff in a stripper solution (Microposit Remover 1165) and sonicated gently for a few minutes to get a clean liftoff.

3.3 Graphene Transfer

Our approach to transfer graphene from the copper sheet to the device substrate is inspired from the SPeeD technique [46]. This technique exploits the hydrophilic copper and hydrophobic graphene interface interactions. DI water penetrates the interface and thus effectively separates the copper from the graphene. We have of course optimized and significantly altered parameters of the technique to give best results for graphene transfer.

PMMA (8% in Anisole) is spin coated over the CVD grown graphene on copper to a thickness of 500nm. This PMMA-graphene-copper sheet is baked at 170 C for about

5-7 minutes to get rid of unwanted solvents. A thin Kapton tape is then stuck on the PMMA side of this baked sheet and is flattened using a Teflon roller. This flattening is done to ensure a good uniform contact between the PMMA and the tape. The sample is then heated in DI water at 90 C for a period of 90-120 minutes. We note that leaving the sample in DI water overnight and then heating it for 90 minutes enables easier peel off of the copper and thus a better transfer. However, if the sample is not left overnight in water, a period of 120 minutes generally ensures that just the copper and not graphene with copper is peeled off. The process is time dependent in that for times lower than 100 minutes, the copper peeling is not effective while for times of more than 150 minutes, the Kapton loses its adhesive properties at high temperatures and also peels off along with the metal.

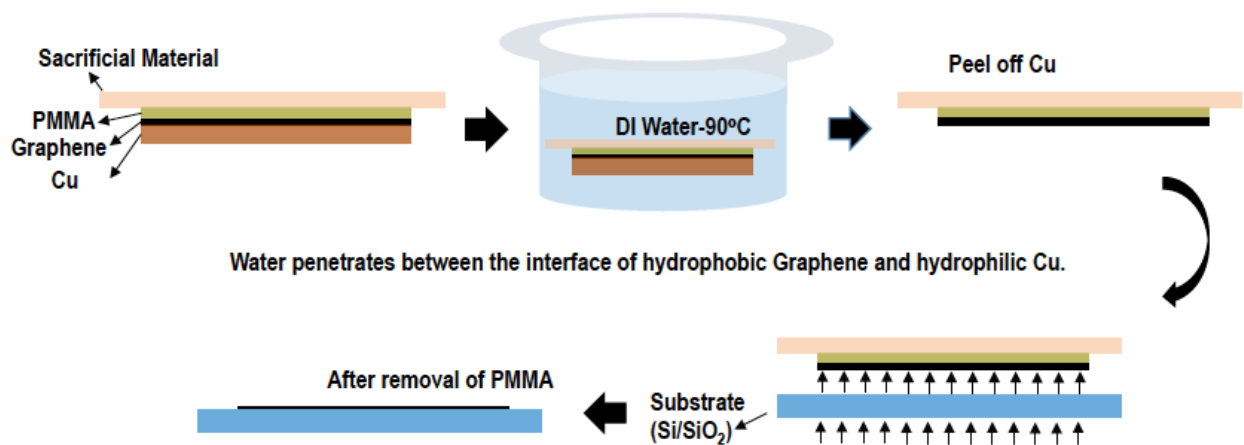


Figure 6 Schematic Illustration of Contamination Free Graphene Transfer Technique

This method of using a Kapton tape still leaves some residual particles mixed with PMMA that are notoriously difficult to remove. Therefore, we have also used other materials like PDMS [50] and a suitable gel (Gel-Pak DGL gel film) [51] that result in a cleaner surface. We have since optimized the heating time and temperature for

these materials in water. Since the use of such a material, be it Kapton tape or PDMS or the DGL gel, is just to provide support and a smooth surface before the copper is peeled off and is later discarded, we simply refer to these materials as the 'sacrificial material' (SM). The choice of the SM does not affect graphene properties.

The sample is then taken out of DI water. Immediately after, but very slowly, the copper is peeled off using a set of pointed tweezers. A drop of water is put on the graphene side of the SM-PMMA-graphene sample and the sample is then gently lowered onto the pre-fabricated devices in between the source and drain contacts in the array of inter-digitated electrodes. The graphene-PMMA-SM can further be glided onto any desired location without loss in graphene quality because of the use of this water-drop technique. The sample is then left overnight for the water to dry out. Later, the device with the graphene-PMMA-SM on it is baked at 140C for 45-60 minutes. This gets rid of residual moisture but also melts the PMMA. Now the sample is immersed in acetone for a period of 10 minutes whereupon, the molten PMMA along with the SM above it separates from the device that is left with just a graphene channel between the source and the drain.

We note that the gradual evaporation of water-drop ensures uniform contact between the graphene and the device substrates. We have observed that the contact quality is worse if we immediately bake the device to get rid of the water. We also feel it important to mention that the process is independent of the size of the graphene to be transferred and can thus be scaled to arbitrary areas.

Also, it is important to report that we have successfully observed Dirac Points on the device even before the SM was separated from the device. In principle, the graphene channel FET works as soon as a good contact between graphene and substrate is ensured. However, functionalization of graphene surface requires the graphene to be as clean as possible to ensure higher sensitivity and better signal to noise ratio. To clean the graphene of any residues, the following steps were performed.

After separating the SM-PMMA from the graphene FET, the device was left in acetone for 20-25 minutes and sonicated to clean PMMA residues. The device was cleaned with isopropanol (IPA) to remove acetone residues and then with DI water. Later, the device was heated in stripper solution (Microposit Remover 1165) at 80 C for 90 minutes and left to cool overnight. The device was again cleaned with IPA and DI water. Finally, the device was vacuum annealed at 300 C for 3 hours in order to get a very clean graphene surface in keeping with reported literature [52].

We note that all chemical treatment and processing is done before graphene is transferred onto the wafer. This is in contrast to other experiments on graphene when graphene was first transferred onto the substrate and then the metal electrodes were patterned onto it [6,44]. This is done because the copper etching technique for graphene transfer does not have good control over exact location of graphene transfer and so, the source and drain contacts are aligned to wherever the graphene channel exists. However, we adopt variants SPeeD technique, which gives precise spatial control over the transfer size, area and location. Furthermore the transfer of graphene onto the FET is done without exposing graphene to any harsh chemicals that

uncontrollably or unintentionally dope the graphene. Such doping alters the electrical properties of graphene and is the suspected reason behind observance Dirac Points at unexpected voltages.

3.4 Metal Insulation

As mentioned earlier, the source and drain electrode have to be protected from the aqueous environment. In order to insulate the metal, we spin coated a negative tone resist (nLOF 2020 from AZ Electronic Materials) over the device. We then opened a window using lithography and exposed the source and drain metal electrodes to the aforementioned MA6 aligner. Time of exposure was deliberately kept longer than before so that a little overexposure resulted in resist remaining about $0.5\mu\text{m}$ to $1\mu\text{m}$ on either side of the electrode. This ensured that the sidewalls of the metal electrodes were also insulated by the resist. The resist was developed in tetramethylammonium hydroxide (TMAH) solution. After development, only the locations of the graphene channel are exposed to the atmosphere while the rest of the electrodes are protected.

We realize that now we have exposed our pristine graphene surface to doping through the use of TMAH. However, as opposed to the previous chemical treatments, effects of graphene doping due to TMAH have been well documented [53]. TMAH negatively dopes the graphene reducing the Dirac Point voltage when tested via back gating. The rate of shift of voltage has also been found to be about 1V/sec for TMAH. Consequently, either a new offset can be created at this voltage or the graphene can be rinsed in DI water and hard baked till the Dirac Point reappears at the pre-TMAH voltages. These approaches give the same results when the graphene is functionalized.

An additional advantage of hard baking the device after covering the metal with the resist is that the resist hardens and is not easily peeled. This is extremely advantageous for repeatability of devices. A schematic illustration of the GraFET device is shown in Figure [6].

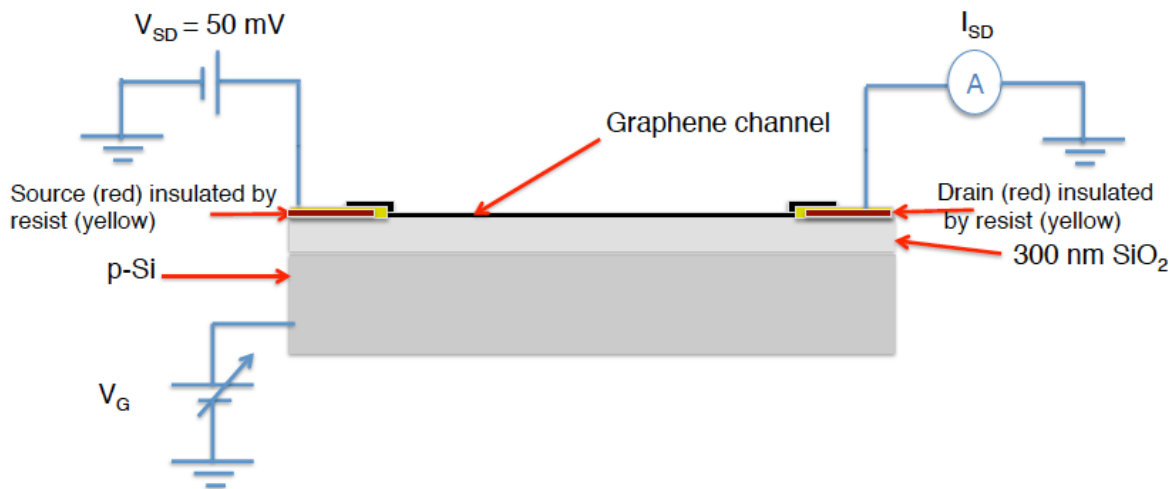


Figure 7 Schematic of Final GraFET Device along with Details of Characterization

We note that as previously mentioned one of the primary criteria in the present device design is ease of use. However, since this approach requires covering the metal and subsequent treatment with TMAH, we propose an alternate design as follows. After the graphene surface is cleaned, a PDMS based microfluidic channel with width corresponding to the width of the graphene channel ($\sim 50\mu\text{m} - 100\mu\text{m}$) can be easily fabricated and aligned with the channel. If the solution to be tested for protein detection is now flowed through this channel so that the solution is restricted by the PDMS and comes into contact with only the graphene, the device can be tested without exposure to any chemical that involves the risk of affecting the electrical properties of graphene. This modification is trivial and furthermore we get excellent sensing response with the current

approach as shown in Chapter 4. Therefore, while recognizing that the microfluidic channel based approach may be better suited for other proteins or biomolecules, for our purposes in sensing BSA and Lysine, this approach is put on hold.

3.5 Device Testing

The final device was characterized via I-V measurements in order to test for continuity of channels and to measure the resistance of graphene as well as the contact resistance. During the I-V test, the source-drain voltage was varied whilst measuring the drain current. To observe the Dirac Point, a gate voltage sweep was conducted keeping the drain voltage constant. A plot of Drain Current vs. Gate Voltage shows the gating characteristics of the device including the charge neutrality (Dirac) point. All measurements were taken using a probe station set up consisting of two source measurement units (SMUs) from Keithley Instruments. For all gating experiments, we applied a gate voltage through the back-gate mechanism and for these measurements the source-drain bias voltage was constant at 50mV.

To detect specific proteins, the device was dipped in a pre-determined concentration of the protein for a pre-determined amount of time. The liquid was blow dried gently off the surface and a similar I-V and gating test was performed. The protein solution was just the specific protein dissolved in DI water in pre-determined amounts. To confirm that effects of protein and not a placebo effect of just DI water on graphene was being observed, an offset was given to the data to place the origin at the point where the graphene FET was exposed to just DI water (zero protein concentration). When non-zero protein concentrations were use, changes in the Dirac point with respect

to this point because of the graphene functionalization due to the protein were noted. These results are presented in Chapter 4. To revert the device back to its original state, the device was rinsed thoroughly in DI water for a long time and then baked for a few minutes to drive out moisture.

Chapter 4

Results and Discussion

4.1 Graphene Growth Characterization

4.1.1 Simple Oxidation Test

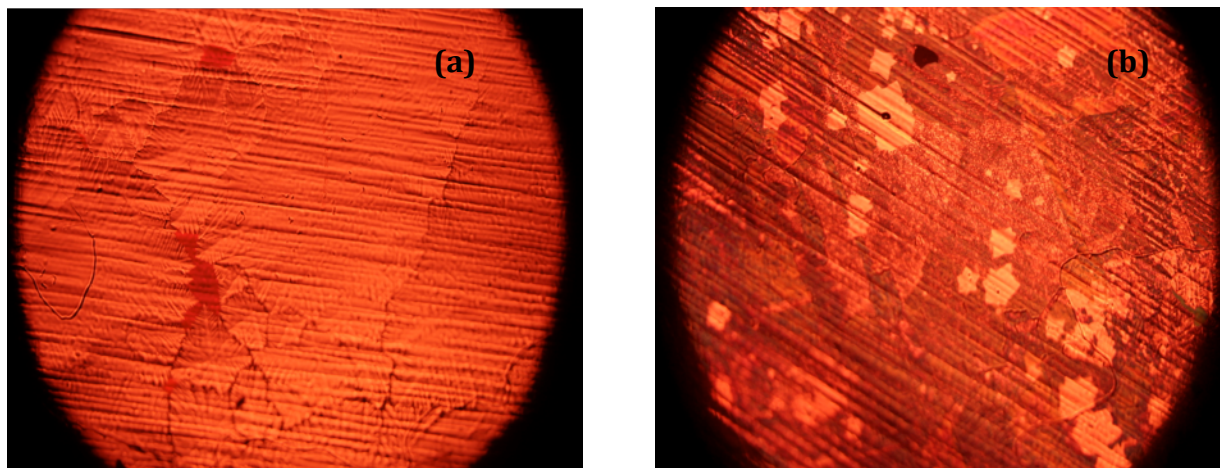


Figure 8: Post-oxidation CVD graphene/copper (a) bare oxidized copper and (b) bright graphene patches that prevent oxidation on oxidized copper

A simple oxidation test, wherein the graphene on copper sample is heated at 250C for a few seconds gives a quick indication to the quality of growth. Copper at such high temperatures oxidizes to red colored oxide while graphene is not affected because of the similar heat treatment. So, if a copper sample partially covered by graphene is heated, only those parts which are bare copper get oxidized and turn red while patches where the graphene layer protects the copper underneath it do not change color. Figure [8] shows this contrast when looked at under an optical microscope. It is also worthwhile to note the hexagonal shape of graphene grains take upon nucleation. An estimate of grain size can also be made using this quick and easy technique. When a uniform layer

of graphene covers the copper, no change in color is observed. Only such samples that have no contrast differences were used on devices.

4.1.2 Scanning Electron Microscope Imaging

A. Partial Growth

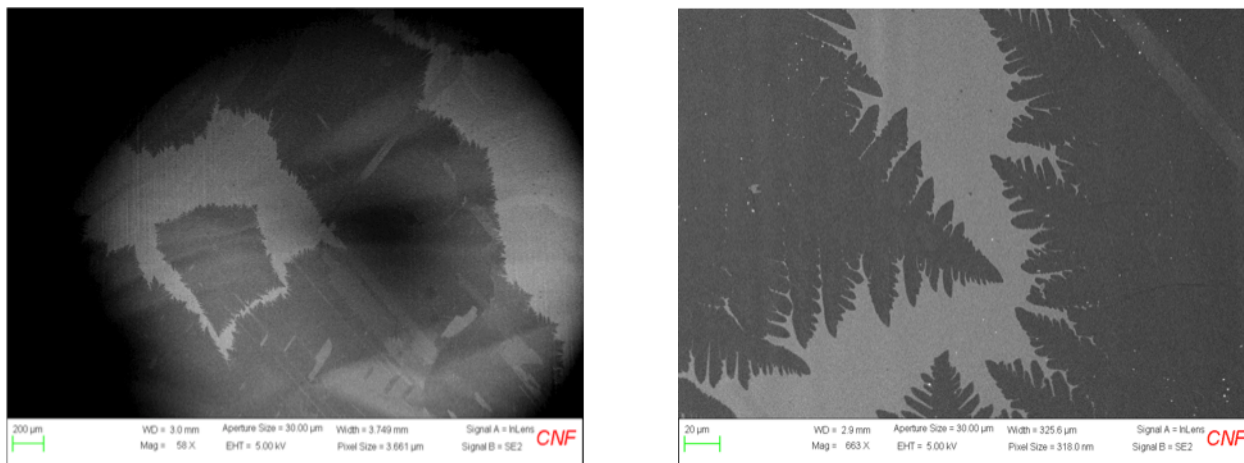


Figure 9 (a) SEM image of Partial or patchy growth of graphene and (b) close up view of patch of graphene showing feather like edge between graphene and copper

While the oxidation test gives a rough idea about the presence of a protecting layer above the copper, confirmation that the layer has uniform coverage and is monolayer was obtained through scanning electron microscopy. Figure [9] shows a partial or patchy growth of graphene on copper. The contrast between graphene monolayer and bare copper is clear and the feather like indentations as observed in Figure [9b] are an indicator of the presence of graphene as opposed to other possible forms of carbon.

B. Multilayered Growth

A multilayered growth is also easily detected in SEM images as shown in Figure [10]. The contrast between the high degree of multi layer patches and the surrounding

monolayer graphene are seen distinctly. We note that the multilayer patches correspond to nucleation sites as expected. Samples of graphene that are heavily multilayer were also ignored as the presence of multiple layers introduces a band gap in the graphene [54]. This uncontrolled band gap leads to the disappearance of the Dirac Peak and is thus not useful for sensing purposes.

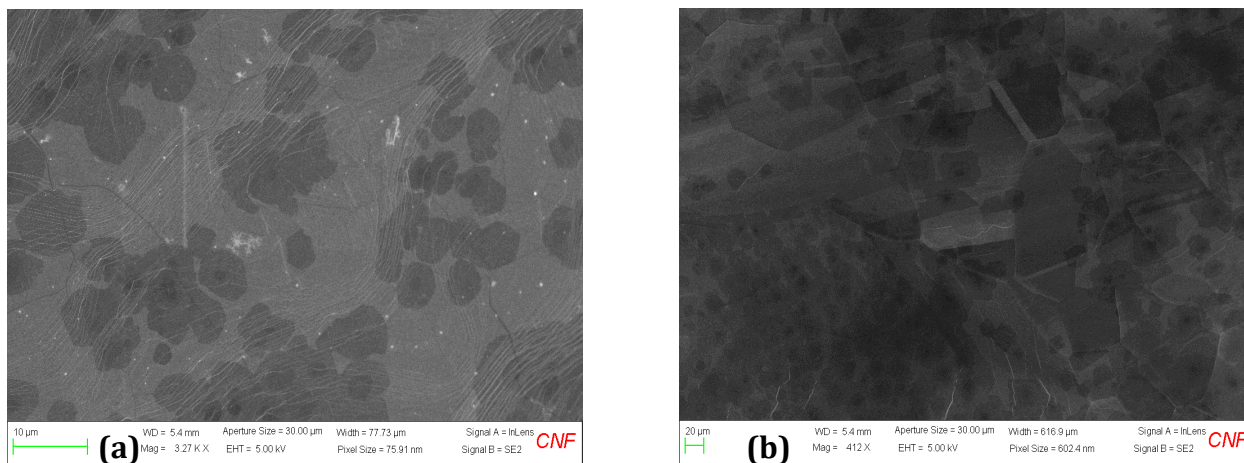


Figure 10 SEM images of (a) standard and (b) pita pocket multilayered graphene growth

C. Single Layer Graphene

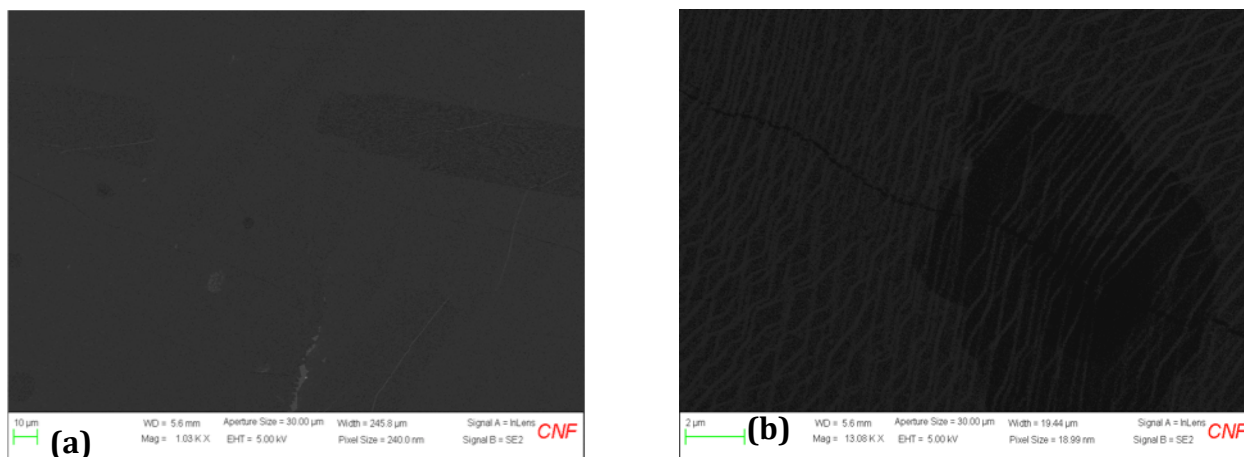


Figure 11 Single layer graphene (a) uniform coverage (b) small characteristic sand dune like features in graphene monolayer. No contrast is observed for graphene monolayer and so a uniformly dark region is seen for most part through the SEM

As opposed to such images, single layer graphene shown in Figure [11] shows an almost uniform contrast indicating a uniform coverage of the copper substrate by monolayer graphene. The distinctive sand dune like pattern as in Figure [11b] for monolayer graphene is observed many times and is attributed either small rips in the graphene which have negligible effect on the electrical properties of graphene. The rips also tend to be concentrated towards areas that are less smooth and so the relatively flat areas of graphene as shown in Figure [11a] that do not have the sand dune patterns are selected for transfer onto devices.

4.1.3 Raman Spectrum

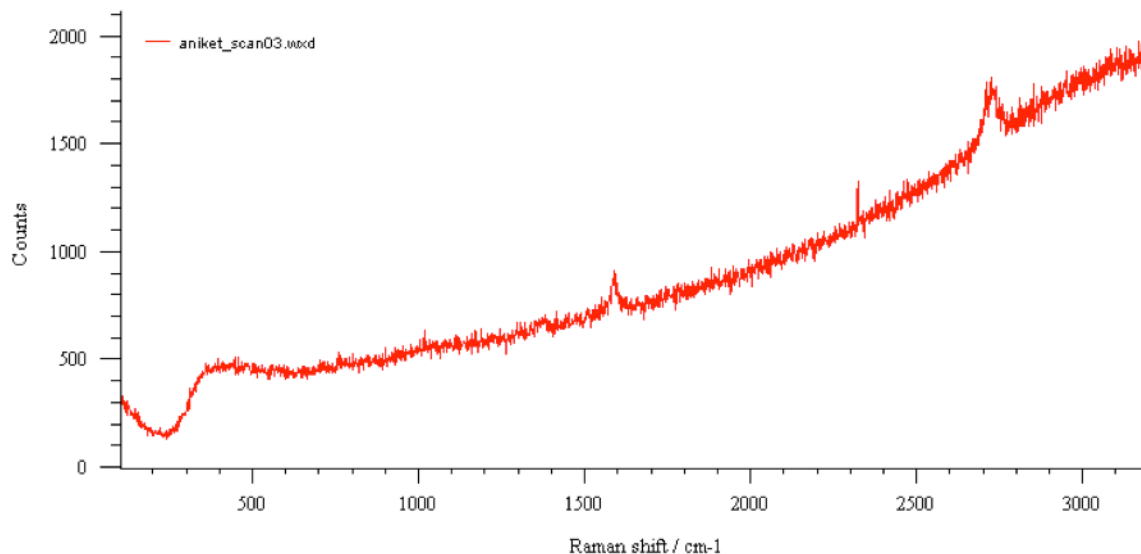


Figure 12 Raman spectrum of graphene with G and 2D peaks on characteristic copper background spectrum

Finally to confirm that the monolayer on the copper substrate is indeed a graphene single layer and not amorphous soot from the growth furnace, a Raman spectrum of the graphene on copper is taken. This is shown in Figure [12]. The increasing background is common for copper and the existence of graphene is

confirmed through the presence of G and 2D peaks at 1580 cm^{-1} and 2690 cm^{-1} respectively [55].

4.2 GraFET Characterization

4.2.1 I-V Characteristics of GraFET devices

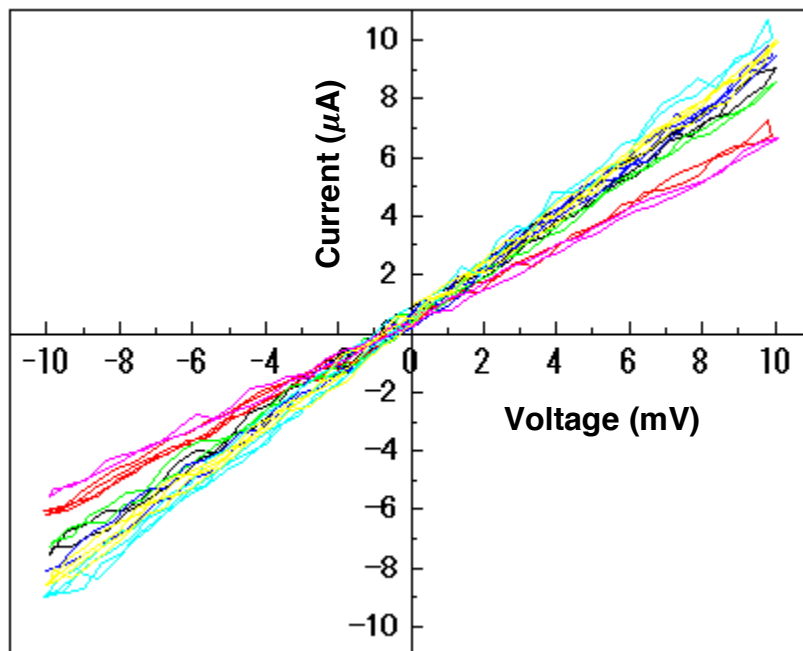


Figure 13 I-V characteristics of GraFET devices

The drain current vs. source-drain voltage (I-V) characteristics of the GraFET device are linear as expected. This is shown in Figure [13]. The linear I-V curves demonstrate success of graphene transfer by our novel approach. In absence of graphene there is no electrical connection between the electrodes as the metal electrodes are on a 300nm thick layer of insulating oxide. The I-V characteristics without graphene are thus just open circuit noise. We also note that for the different individual devices on a single chip, the I-V curves are very similar. This indicates that the contact

between the graphene and metal electrodes is good and also that the channel material is largely homogenous throughout.

4.2.2 Resistance Measurements of GraFET devices

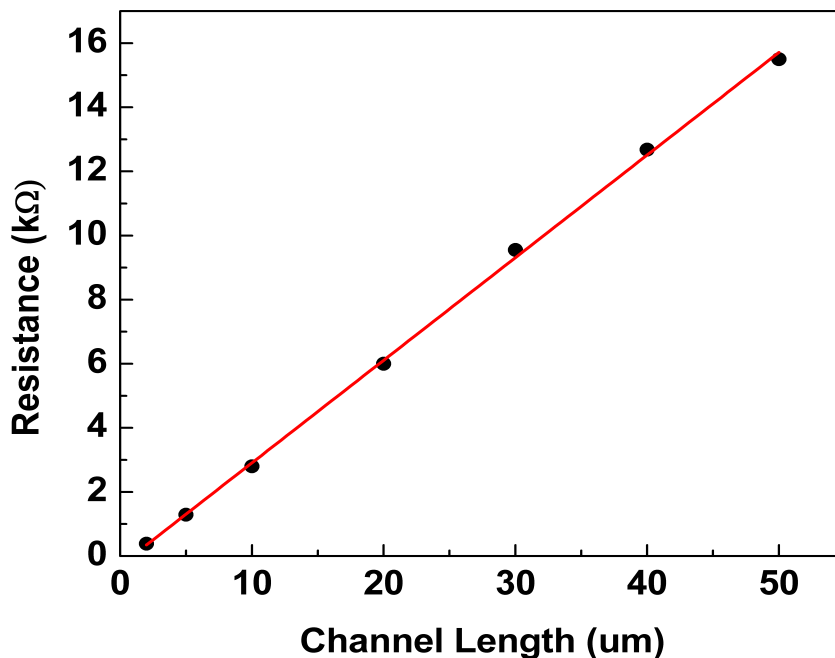


Figure 14 Contact Resistance extraction for GraFET devices

As graphene is a 2D material, sheet resistance or resistance per square meter takes the place of normal bulk resistance. This sheet resistance also depends on the ratio of length and width of graphene and for our typical samples the ‘R per square’ was about $4\text{k}\Omega/\text{sq}$. Our chip design that consists of device arrays of channel lengths varying from $5\mu\text{m}$ to $150\mu\text{m}$ was used to calculate the contact resistance between metal and graphene. Figure [14] shows a plot of resistance vs. channel length, which when extrapolated to a zero channel length gives twice the contact resistance. Our devices

show negligible contact resistance ($\sim 100 \Omega$), which is excellent when, sheet resistance of $\sim 4 \text{ k}\Omega/\text{sq.}$ is observed.

4.3 Demonstration of Dirac Point and its Tunability

We observe Dirac Points for our devices when in air. Till the metal has not been insulated the graphene has not been exposed to any sort of chemical that may alter its electrical properties. Specifically, no ionic dopants have been introduced because of etching with ferric chloride or the likes. The Dirac point for such devices with CVD graphene is found to be $\sim 25\text{-}30\text{V}$. This is shown in Figure [15] by the red curve. The Dirac Point at non-zero voltage even though graphene has not been exposed to any chemicals might surprise some, but to us this effect was but expected. The effect of the substrate on graphene and Dirac Peak has already been shown by B. Kumar et al. [56]. We use highly p-doped silicon wafer as a substrate for our devices. Use of such p-silicon enhances conductivity of the silicon that helps during back gating. We note that the silicon doping is highly controlled and so this effect is simply equivalent to giving an offset of $20\text{-}25 \text{ V}$ from zero volts. Furthermore, we have recycled devices and this opens up the possibility of the silicon oxide trapping charges or defects that further alter the original Dirac Point of graphene. We suspect this is the main reason that the Dirac Point is not at an exact voltage but ranges from $\sim 20\text{-}25\text{V}$. Such a straggle will be eliminated if a fresh and pristine oxide and substrate is used for each device. We note that previously, Dirac points near 0V have been reported, but these are on devices that transfer graphene first and then pattern the metal electrodes on top. This involves use of a developer solution like TMAH that dopes graphene negatively. We suspect such

exposures might be responsible for decreasing the Dirac Point from the 20-25 V range to near 0V range.

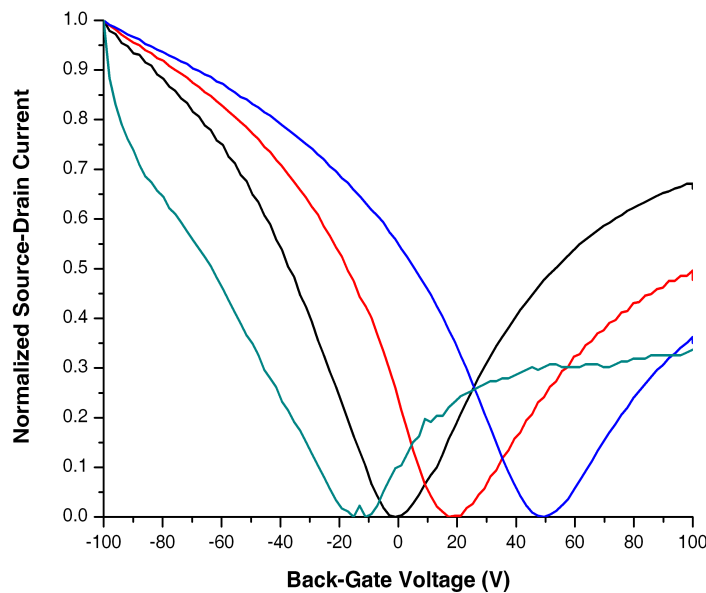


Figure 15 Red curve - Dirac Point of GraFET device not exposed to any chemical. Blue - GraFET treated with methylene chloride. Black - GraFET treated with TMAH once and Green - treated with TMAH twice.

Evidence for this claim is obtained through Figure [15]. We can tune the Dirac Point of graphene once the metal electrodes have been covered for large range of back gate voltages, both positive and negative. Figure [15] shows a few typical plots at positive, near zero and negative voltages. Graphene in these devices has been exposed to the developer TMAH and methylene chloride solutions. TMAH can be used to lower the Dirac Point voltage while methylene chloride can be used to raise it. We have quantified the shift in Dirac Point because of TMAH to be at a rate of 1V/sec towards lower voltages and thus can tune Dirac Points at desired voltages. The

methylene chloride was used only here to demonstrate that the Dirac Point could be tuned to a desired value. As graphene was never exposed to methylene chloride in an actual device that was used for bio-sensing, we have not extensively studied the effects of methylene chloride on graphene except that it shifts the Dirac Point to higher voltages. We note, that thorough rinsing in DI water for prolonged time intervals followed by hard baking for 30-45 minutes restores the Dirac Point to near original values of ~20-25 V. Devices were extensively tested to yield a stable Dirac Point prior to detecting specific proteins.

4.4 Specific Biomolecule Detection

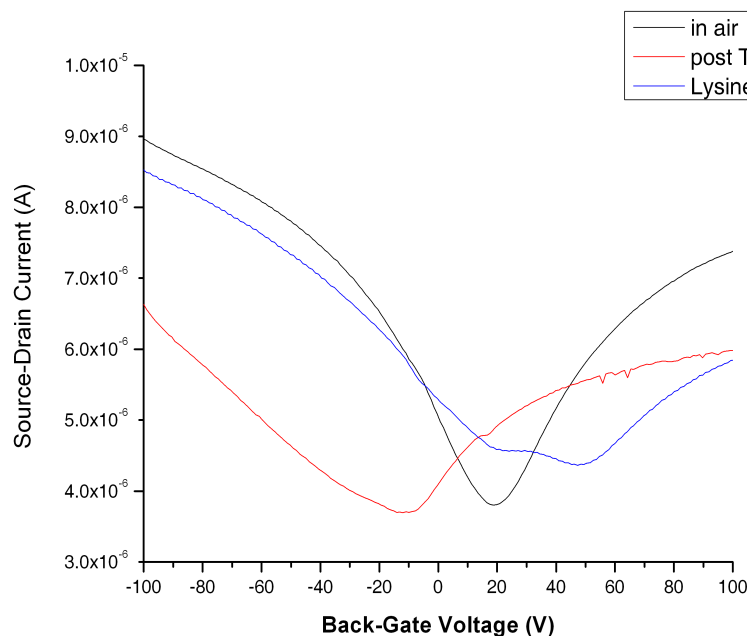


Figure 16 Detection of Lysine using GraFET device

We have successfully fabricated graphene channel field effect transistors. The process of transferring graphene from copper substrate onto the FET is contamination free and gives precise control over position where the graphene channel is located. Device fabrication is mostly done prior to graphene transfer thus avoiding exposing

graphene to many of the harsh chemicals. Furthermore, CVD grown graphene was used and the process is scalable to arbitrary large areas. The graphene surface was functionalized using two specific proteins namely lysine and bovine serum albumin (BSA).

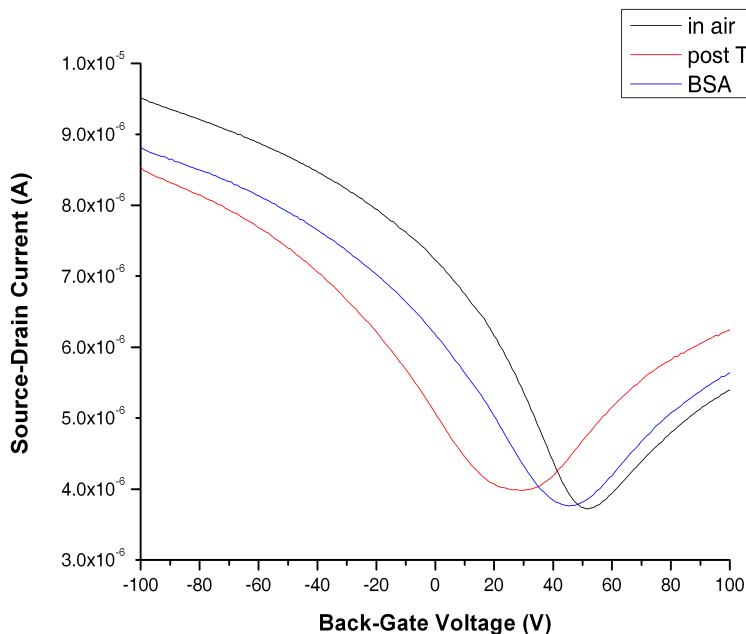


Figure 17 Detection of BSA using GraFET device

When the GraFET device was exposed to specific protein environments, signature shifts in Dirac Point of the GraFET device were observed. This shift in the Dirac Point is exploited and our GraFET devices are used to sense and detect specific protein biomolecules.

Figure [16] shows the shift in Dirac Point in our GraFET device due to functionalization through lysine while that due to BSA is seen in Figure [17]. The observed shift is because the graphene surface is functionalized leading to a change in

the number of carriers in graphene and thus a shift in its Dirac Point. Such a change in the number of carriers is caused because the protein biomolecules carry a charge which interacts with the graphene when the biomolecules adsorb non-covalently onto the graphene surface. The charge transfer and the degree of adsorption of molecules onto same areas of graphene are highly protein specific and so, the shift in Dirac Point is a signature of every biomolecule. Our GraFET can thus be used as an effective bio-electronic sensor. We note that the shifts in the Dirac Point during protein detection are quite large, making it an easy to use biosensor.

4.4.1 Mechanism behind Functionalization – Langmuir Model

To investigate and confirm the mechanism governing the functionalization, we performed tests with varying the concentration and time parameters for both BSA and lysine. These data points are offset to have Dirac Point in DI water as reference. We note that this point should ideally be the same as that in air but in practice these are a little different. We attribute this effect to moisture penetrating the porous resist covering the metal. A small metal/solution interaction is not ruled out, though this effect is negligible as compared to the effect because of functionalization.

Fig [18a] shows a plot of the shift in the Dirac Point with time (number of seconds device is dipped in protein solution for functionalization) at specific concentrations (40nM) for lysine. Figure [19a] shows the same for BSA. We see that binding reaches equilibrium and stabilizes for $t > 30$ sec. This implies that dipping the device in protein solution achieves nearly the full extent of binding that may be achieved at equilibrium conditions during graphene functionalization because of the protein. These time scales

(t ~30 sec) have been used in subsequent experiments. We note that functionalization due to lysine reaches equilibrium quicker than due to BSA. Such differences along with the signature shifts make our GraFET devices excellent bio-electronic sensors.

Figure [18b] shows a plot of the shift in the Dirac Point with varying concentrations of lysine. Figure [19b] shows the same for BSA. At each concentration, we left the protein for enough time durations to let near complete functionalization occur. From this experiment, the dissociation constant of the binding reaction can be obtained.

From Figure [18b] and Figure [19b] the non-covalent

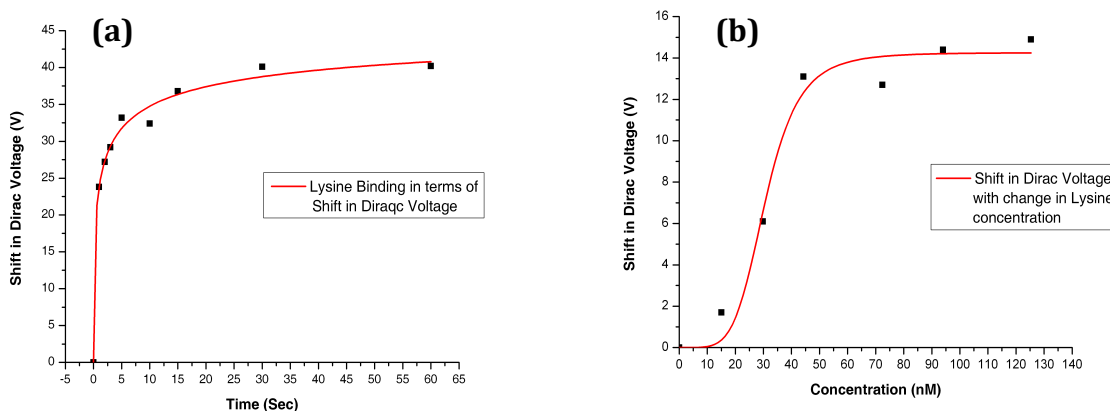


Figure 18 Graphene functionalization through Lysine - (a) shift in Dirac Point at 40nM concentration and (b) evidence of Langmuir adsorption for Lysine functionalizing graphene

functionalization is seen to follow the Langmuir adsorption curve [57]. K_D , the dissociation constant for this reaction is calculated from this plot. To get this value of K_D the data is fit to the Hill equation [58] as shown by the red curve in Figure [17b] and Figure [18b]. The Hill equation is $V_{eqm} = V_{max} * \frac{1}{1 + \left(\frac{K_D}{[biomolecule]}\right)^h}$ where V_{eqm} and V_{max} are equilibrium and maximum shifts in the voltage, K_D is the dissociation constant and h is a fitting parameter and $[biomolecule]$ is the concentration of the biomolecule to be

detected. Extracted values of K_D for BSA and lysine are $\sim 12\text{nM}$ and 32nM respectively. The value of h is ~ 1.9 for BSA and ~ 5.1 .

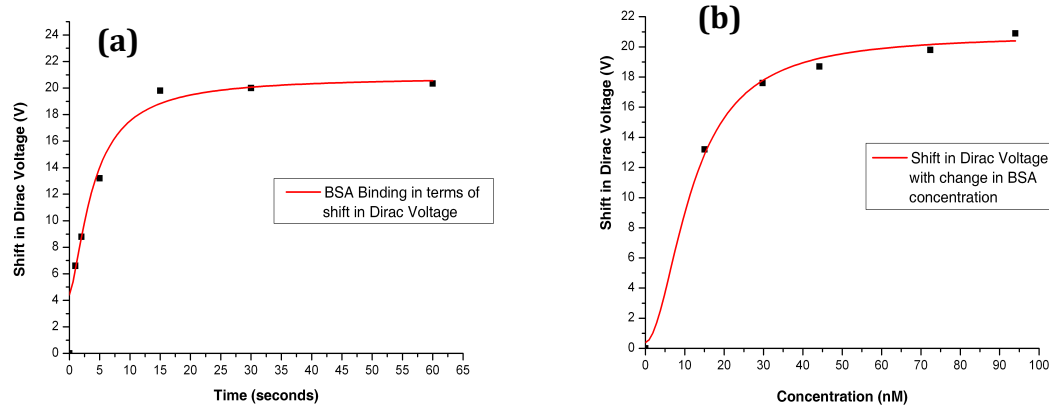


Figure 19 Graphene functionalization through BSA - (a) shift in Dirac Point at 40nM concentration and (b) evidence of Langmuir adsorption for BSA functionalizing graphene

4.5 An Array of GraFET Sensors

Our device design and detection technique allows an array of sensing GraFET devices to be fabricated onto a single chip. These may be made with identical or varying channel lengths. We accommodate as many as 26 individual sensing GraFET devices onto a single mini-chip. For use in bio-sensing applications, considering that as many as 8 mini-chips may be fabricated on a single 4" wafer, we see that our devices already take a step towards moving from the purely academic world to the commercial world. Alternatively, in the lab-on-a-chip approach, if a single mini-chip of GraFET devices is accommodated on a single chip, parallel detection of more than 25 biomolecules is potentially possible, thus enabling high throughput applications. As long as the same piece of graphene is used as channel material in all of the individual devices, we

observe similar Dirac Points across the array. This is shown in Figure [20]. Even for varying channel lengths, almost the same Dirac Point is observed.

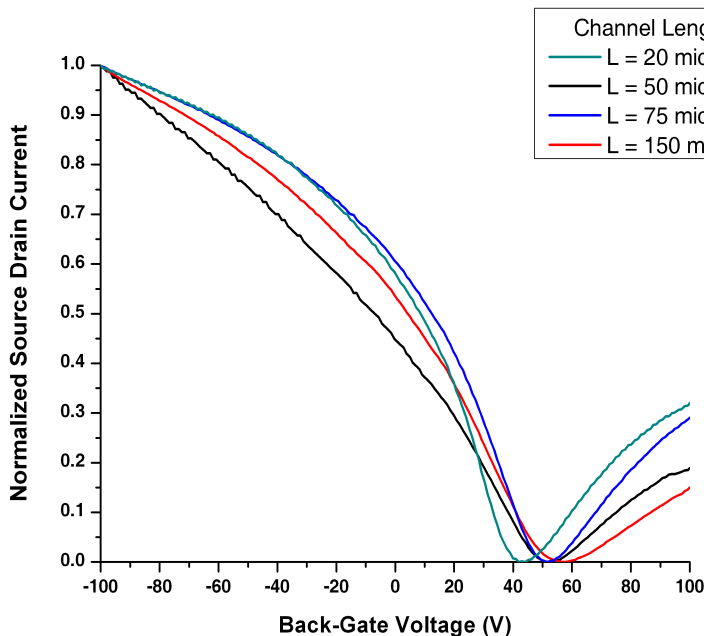


Figure 20 An Array of GraFET sensors

The data is normalized to account for differing currents as channel width varies. This functionality of our devices enables multiple biomolecules to be potentially detected using just a single chip. For this, the only modification to be done is that the biomolecule containing solution that functionalizes the graphene should be restricted on a particular device. This can be done using a microfluidic channel approach as explained earlier. A high-throughput device is then achievable. However, our fundamental goal being demonstrating large shifts in the Dirac Point because of bio-functionalization of graphene, we have stopped at analyzing one biomolecule at a time using the metal insulation approach.

We also note that the device is repeatable until the resist covering the metal does not peel off. In our experience, a single device lasts for about 15 – 20 cycles of protein

testing. However, we hard bake the device when we need to restore it to its initial conditions. During this process the resist hardens and even if some part of it peels off, the remnant resist can only be removed using harsh resist stripper solutions that get rid of the graphene as well. Of course, source and drain electrode arrays are still functional after this in that another sample of piece of graphene may be transferred onto them and the GraFET is good to go.

Chapter 5

Conclusions and Future Work

5.1 Conclusions

Our results are evidence of functionalization of graphene because of biomolecules. Signature shifts in the Dirac Point have been used to detect specific biomolecules successfully. The protein biomolecules have a non-covalent binding interaction with graphene. The adsorption of these proteins is controlled through Langmuir adsorption. The corresponding rate is calculated to be $\sim 32\text{nM}$ for lysine and 12nM for BSA. Parallel detection of multiple biomolecules is also possible with slight modifications to our GraFET devices.

The shift in Dirac Point is of the order of volts, often tens of volts, which is much more than previously observed for similar protein concentrations. We attribute the greater amounts of shift attributed to quality of graphene but more importantly large areas of extremely clean and uncontaminated graphene. The large signature shifts in Dirac Point helps detect particular biomolecules and the functionalized graphene channel in the FET is thus a platform for biomolecule sensing and detection. The GraFET devices can be easily a part of the lab-on-a-chip approach that bioelectronics is moving towards. In addition to the enhanced sensitivity, our GraFETs also have an advantage of being easier to use for the end-user.

Our GraFET sensor devices are reversible in that they revert back to their original state by just rinsing thoroughly in DI water, drying and heating to remove remnant

moisture. Additionally, an array of such sensors is fabricated on each device. These multiple individual devices on a single chip make possible the detection of various proteins on a single batch of graphene thus removing any offset errors arising because of differences in quality of graphene. All such qualities coupled with the inherently large signature Dirac Point shifts due to bio-functionalization of the graphene make our GraFET devices excellent bio-electronic sensors.

5.2 Scope for Future Work

We have suggested the use of PDMS based microfluidic channels as a means of totally eliminating exposure of graphene to any chemicals at all, leaving the graphene channel surface pristine when interacting with biomolecules. Implementation of this approach may be worthwhile as we expect a cleaner set of data with the possibility of increased sensitivity because of totally uncontaminated graphene. Additionally, because a single chip contains multiple working devices properly designed channels open the possibility of simultaneous detection of numerous biomolecules on the same sample of graphene. This would be a significant step in reaching the lab-on-a-chip stage as far as specific biomolecule detection is concerned.

Another possibility is the use of alternative approaches to functionalization through the use of tripod anchor molecules [59]. Such molecules are claimed to increase the time for which graphene remains functionalized and it remains an interesting topic worth investigating in detail especially with our large area, array of sensor devices.

REFERENCES

1. Heath, James R., Mark E. Davis, and Leroy Hood. "Nanomedicine targets cancer." *Scientific American* 300.2 (2009): 44-51.
2. Humayun, Mark S., et al. "Visual perception in a blind subject with a chronic microelectronic retinal prosthesis." *Vision research* 43.24 (2003): 2573-2581.
3. Shah, Samip, et al. "Electrical properties of retinal–electrode interface." *Journal of neural engineering* 4.1 (2007): S24.
4. Offenhäusser, Andreas, et al. "Field-effect transistor array for monitoring electrical activity from mammalian neurons in culture." *Biosensors and Bioelectronics* 12.8 (1997): 819-826.
5. Patolsky, Fernando, et al. "Detection, stimulation, and inhibition of neuronal signals with high-density nanowire transistor arrays." *Science* 313.5790 (2006): 1100-1104.
6. Hess, Lucas H., Max Seifert, and Jose A. Garrido. "Graphene transistors for bioelectronics." *Proceedings of the IEEE* 101.7 (2013): 1780-1792.
7. Allen, Brett Lee, Padmakar D. Kichambare, and Alexander Star. "Carbon Nanotube Field-Effect-Transistor-Based Biosensors." *Advanced Materials* 19.11 (2007): 1439-1451.
8. Steinhoff, Georg, et al. "Recording of cell action potentials with AlGaIn/GaN field-effect transistors." *Applied Physics Letters* 86.3 (2005): 033901-033901.
9. Kula, Tapas, et al. "Recent advances in graphene-based biosensors." *Biosensors and Bioelectronics* 26.12 (2011): 4637-4648.
10. Hess, Lucas H., et al. "Graphene transistor arrays for recording action potentials from electrogenic cells." *Advanced Materials* 23.43 (2011): 5045-5049.
11. Cohen-Karni, Tzahi, et al. "Graphene and nanowire transistors for cellular interfaces and electrical recording." *Nano letters* 10.3 (2010): 1098-1102.
12. Geim, Andre K., and Konstantin S. Novoselov. "The rise of graphene." *Nature materials* 6.3 (2007): 183-191.
13. Geim, Andre Konstantin. "Graphene: status and prospects." *science* 324.5934 (2009): 1530-1534.
14. "The Nobel Prize in Physics 2010". *Nobelprize.org*. Nobel Media AB 2013. <http://www.nobelprize.org/nobel_prizes/physics/laureates/2010/>
15. Sutter, Peter. "Epitaxial graphene: How silicon leaves the scene." *Nature Materials* 8.3 (2009): 171-172.
16. Dobkin, Daniel Mark, and Michael K. Zuraw. *Principles of chemical vapor deposition*. Dordrecht, The Netherlands: Kluwer academic publishers, 2003.
17. Liu, Zhibo, et al. "Nonlinear optical properties of graphene oxide in nanosecond and picosecond regimes." *Applied Physics Letters* 94.2 (2009): 021902.
18. Zhang, Z. Z., Kai Chang, and F. M. Peeters. "Tuning of energy levels and optical properties of graphene quantum dots." *Physical Review B* 77.23 (2008): 235411.
19. Balandin, Alexander A. "Thermal properties of graphene and nanostructured carbon materials." *Nature materials* 10.8 (2011): 569-581.

20. Balandin, Alexander A., et al. "Superior thermal conductivity of single-layer graphene." *Nano letters* 8.3 (2008): 902-907.
21. Lee, Changgu, et al. "Measurement of the elastic properties and intrinsic strength of monolayer graphene." *science* 321.5887 (2008): 385-388.
22. "The 2010 Nobel Prize in Physics – Press Release". Nobelprize.org. Nobel Media AB 2013. <http://www.nobelprize.org/nobel_prizes/physics/laureates/2010/press.html>
23. Charlier, J-C., et al. "Electron and phonon properties of graphene: their relationship with carbon nanotubes." *Carbon nanotubes*. Springer Berlin Heidelberg, 2008. 673-709.
24. Semenoff, Gordon W. "Condensed-matter simulation of a three-dimensional anomaly." *Physical Review Letters* 53.26 (1984): 2449-2452.
25. Kittel, Charles, and Paul McEuen. *Introduction to solid state physics*. Vol. 8. New York: Wiley, 1986.
26. Schmidt, Charles. "The bionic material." *Nature* 483.7389 (2012).
27. Heller, Iddo, et al. "Charge noise in graphene transistors." *Nano letters* 10.5 (2010): 1563-1567.
28. Georgakilas, Vasilios, et al. "Functionalization of graphene: covalent and non-covalent approaches, derivatives and applications." *Chemical reviews* 112.11 (2012): 6156-6214.
29. Kuila, Tapas, et al. "Chemical functionalization of graphene and its applications." *Progress in Materials Science* 57.7 (2012): 1061-1105.
30. Ohno, Yasuhide, Kenzo Maehashi, and Kazuhiko Matsumoto. "Label-free biosensors based on aptamer-modified graphene field-effect transistors." *Journal of the American Chemical Society* 132.51 (2010): 18012-18013.
31. Hamilton, Christopher E., et al. "High-yield organic dispersions of unfunctionalized graphene." *Nano letters* 9.10 (2009): 3460-3462.
32. Bourlinos, Athanasios B., et al. "Liquid-Phase Exfoliation of Graphite Towards Solubilized Graphenes." *Small* 5.16 (2009): 1841-1845.
33. Paulus, Geraldine LC, Qing Hua Wang, and Michael S. Strano. "Covalent electron transfer chemistry of graphene with diazonium salts." *Accounts of chemical research* 46.1 (2012): 160-170.
34. Liu, Haitao, et al. "Photochemical reactivity of graphene." *Journal of the American Chemical Society* 131.47 (2009): 17099-17101.
35. Huang, Xiao, et al. "Graphene-Based Materials: Synthesis, Characterization, Properties, and Applications." *Small* 7.14 (2011): 1876-1902.
36. Kodali, Vamsi K., et al. "Nonperturbative chemical modification of graphene for protein micropatterning." *Langmuir* 27.3 (2010): 863-865.
37. Lopes, Manuel, et al. "Surface-enhanced Raman signal for terbium single-molecule magnets grafted on graphene." *ACS nano* 4.12 (2010): 7531-7537.
38. Cheng, Hung-Chieh, et al. "High-quality graphene p– n junctions via resist-free fabrication and solution-based noncovalent functionalization." *ACS nano* 5.3 (2011): 2051-2059.
39. Schedin, F., et al. "Detection of individual gas molecules adsorbed on graphene." *Nature materials* 6.9 (2007): 652-655.

40. Lu, Ye, et al. "DNA-decorated graphene chemical sensors." *Applied Physics Letters* 97.8 (2010): 083107.
41. Li, Xuesong, et al. "Large-area synthesis of high-quality and uniform graphene films on copper foils." *Science* 324.5932 (2009): 1312-1314.
42. Petrone, Nicholas, et al. "Chemical vapor deposition-derived graphene with electrical performance of exfoliated graphene." *Nano letters* 12.6 (2012): 2751-2756.
43. Mattevi, Cecilia, Hokwon Kim, and Manish Chhowalla. "A review of chemical vapour deposition of graphene on copper." *Journal of Materials Chemistry* 21.10 (2011): 3324-3334.
44. Saltzgeber, Grant, et al. "Scalable graphene field-effect sensors for specific protein detection." *Nanotechnology* 24.35 (2013): 355502
45. Gupta, Priti, et al. "A facile process for soak-and-peel delamination of CVD graphene from substrates using water." *Scientific reports* 4 (2014).
46. Schwierz, Nadine, Dominik Horinek, and Roland R. Netz. "Reversed anionic Hofmeister series: the interplay of surface charge and surface polarity." *Langmuir* 26.10 (2010): 7370-7379.
47. Albumin from Bovine Serum. Sigma-Aldrich, Product Information Sheet Retrieved 5 July 2013
48. Perlman, P., and E. Engvall, "Enzyme linked immunosorbent assay (ELISA) quantitative assay for immunoglobulin." *Immuno Chemistry* 8 (1971): 871-878
49. Lysine. Sigma Aldrich, Product Information Sheet Retrieved March 21, 2014
50. Allen, Matthew J., et al. "Soft transfer printing of chemically converted graphene." *Advanced Materials* 21.20 (2009): 2098-2102.
51. Castellanos-Gomez, Andres, et al. "Deterministic transfer of two-dimensional materials by all-dry viscoelastic stamping." *arXiv preprint arXiv:1311.4829*(2013).
52. Lin, Yung-Chang, et al. "Graphene annealing: how clean can it be?." *Nano letters* 12.1 (2011): 414-419.
53. Brenner, Kevin, and Raghunath Murali. "Single step, complementary doping of graphene." *Applied Physics Letters* 96.6 (2010): 063104.
54. Ohta, Taisuke, et al. "Controlling the electronic structure of bilayer graphene." *Science* 313.5789 (2006): 951-954.
55. Ferrari, A. C., et al. "Raman spectrum of graphene and graphene layers." *Physical review letters* 97.18 (2006): 187401.
56. Kumar, Bijandra, et al. "The Role of External Defects in Chemical Sensing of Graphene Field-Effect Transistors." *Nano letters* 13.5 (2013): 1962-1968.
57. Langmuir, Irving. "The adsorption of gases on plane surfaces of glass, mica and platinum." *Journal of the American Chemical Society* 40.9 (1918): 1361-1403.
58. Hill, Archibald Vivian. "The combinations of haemoglobin with oxygen and with carbon monoxide. I." *Biochemical journal* 7.5 (1913): 471
59. Mann, Jason A., et al. "Preservation of Antibody Selectivity on Graphene by Conjugation to a Tripod Monolayer." *Angewandte Chemie International Edition* 52.11 (2013): 3177-3180.